

Review

Reaction Cycles of Halogen Species in the Immune Defense: Implications for Human Health and Diseases and the Pathology and Treatment of COVID-19

Qing-Bin Lu 

Department of Physics and Astronomy and Department of Biology, University of Waterloo, 200 University Avenue West, Waterloo, ON N2L 3G1, Canada; qblu@uwaterloo.ca

Received: 1 May 2020; Accepted: 10 June 2020; Published: 13 June 2020



Abstract: There is no vaccine or specific antiviral treatment for COVID-19, which is causing a global pandemic. One current focus is drug repurposing research, but those drugs have limited therapeutic efficacies and known adverse effects. The pathology of COVID-19 is essentially unknown. Without this understanding, it is challenging to discover a successful treatment to be approved for clinical use. This paper addresses several key biological processes of reactive oxygen, halogen and nitrogen species (ROS, RHS and RNS) that play crucial physiological roles in organisms from plants to humans. These include why superoxide dismutases, the enzymes to catalyze the formation of H_2O_2 , are required for protecting ROS-induced injury in cell metabolism, why the amount of ROS/RNS produced by ionizing radiation at clinically relevant doses is ~ 1000 fold lower than the endogenous ROS/RNS level routinely produced in the cell and why a low level of endogenous RHS plays a crucial role in phagocytosis for immune defense. Herein we propose a plausible amplification mechanism in immune defense: ozone-depleting-like halogen cyclic reactions enhancing RHS effects are responsible for all the mentioned physiological functions, which are activated by H_2O_2 and deactivated by NO signaling molecule. Our results show that the reaction cycles can be repeated thousands of times and amplify the RHS pathogen-killing (defense) effects by 100,000 fold in phagocytosis, resembling the cyclic ozone-depleting reactions in the stratosphere. It is unraveled that H_2O_2 is a required protective signaling molecule (angel) in the defense system for human health and its dysfunction can cause many diseases or conditions such as autoimmune disorders, aging and cancer. We also identify a class of potent drugs for effective treatment of invading pathogens such as HIV and SARS-CoV-2 (COVID-19), cancer and other diseases, and provide a molecular mechanism of action of the drugs or candidates.

Keywords: respiratory burst; phagocytosis; reactive oxygen species; reactive halogen species; reactive nitrogen species; signaling; antitumor agents; antiviral agents; HIV; COVID-19

1. Introduction

Reactive oxygen species (ROS), including superoxide ($O_2^{\bullet-}$), hydrogen peroxide (H_2O_2) and hydroxyl radical (OH^{\bullet}), are constantly produced from aerobic metabolism of the cell. It is known that OH^{\bullet} is potent but non-selective oxidant, while $O_2^{\bullet-}$ and H_2O_2 are far less reactive. Moreover, increasing evidence shows that H_2O_2 is a necessary signaling molecule in the regulation of a variety of biological processes such as cell proliferation and differentiation, tissue repair, immune cell activation, circadian rhythm, vascular remodeling and aging [1–5]. H_2O_2 is also a signaling molecule of plant defense against pathogens [6].

Rising evidence has also clearly demonstrated the critical physiological role of superoxide dismutases (SOD) in humans and all other mammals, which are the enzymes converting $O_2^{\bullet-}$ into H_2O_2 [7]. For instance, it was observed that genetic knockout of SOD produced deleterious phenotypes in organisms ranging from bacteria to mice [8–11]. Knockout mice lacking Mn-SOD died soon after birth or suffered severe neurodegeneration [8]. Mn-SOD was also shown to be required for protecting ROS-induced injury in O_2 metabolism [11]. Mice lacking cytosolic Cu, Zn-SOD developed multiple pathologies, including liver cancer [9], muscle atrophy, cataracts, and a reduced lifespan [10]. Research on biological action of ionizing radiation (IR) also showed that modifying SOD activity in bacteria reduced the oxygen radiosensitizing effect and that SOD injection following whole body x-irradiation significantly protected mice from lethality [12,13]. Also, active SOD or SOD mimic compounds inhibited IR-induced deleterious effects including transformation assays, bystander effects, normal tissue damage associated with inflammatory responses and fibrosis [14,15]. These studies clearly demonstrated that $O_2^{\bullet-}$ was somehow participating in radiation-induced injury, whereas H_2O_2 (SOD) was required for normal physiological functions. Given that $O_2^{\bullet-}$ is a weak oxidant and the downstream formation of OH^{\bullet} from H_2O_2 is responsible for causing oxidative damage, the precise role of H_2O_2 (or $O_2^{\bullet-}$) in these critical physiological functions is essentially unknown [15].

Respiratory burst is the rapid release of reactive species from different types of cells, particularly myeloid cells (phagocytes) such as neutrophils, monocytes, macrophages, mast cells, dendritic cells, osteoclasts and eosinophils. It is usually utilised in immunological defence. Exposure to ROS or *reactive halogen species* (RHS) or *reactive nitrogen species* (RNS) kills the engulfed pathogens, resulting in pathology of infection. Similar respiratory burst is found when cells are exposed to IR at a clinical radiation dose [15] or when the ozone layer is exposed to ionizing cosmic rays in the polar stratosphere especially in the presence of halogenated molecules (particularly freons, CFCs) [16–19].

Phagocytosis is the process by which a cell uses its plasma membrane to engulf a pathogen, forming an organelle called phagosome. It plays a major role in the *innate immune defence* by effectively killing pathogens. The phagosome then moves toward the centrosome of the phagocyte and fuses with lysosomes, forming a phagolysosome for degradation of pathogens. A phagocyte has various receptors on its surface, including opsonin receptors, scavenger receptors and Toll-like receptors. The widely accepted belief is that phagocytosis is most effective for killing microorganisms (e.g., bacteria), while the *adaptive immune defence*, mainly by lymphocytes, is more important for viral infections. However, increasing evidence has shown that phagocytosis plays a crucial role in killing a variety of intracellular or cytoplasmic viruses ranging from influenza, mumps, measles and rhinovirus to Ebola and HIV, either directly protecting against viral infections in the innate immune defence [20–25] or through the antibody-dependent cellular phagocytosis providing mechanisms for clearance of virus and virus-infected cells and for stimulation of downstream adaptive immune responses by antigen presentation or the secretion of inflammatory mediators [26–28]. Particularly in humoral (adaptive) immunity, B cells upon activation produce antibodies, each of which recognizes a unique antigen and neutralizes a specific pathogen. The binding of antibodies to antigens makes the latter easier targets for phagocytes and gives rise to several protective mechanisms. These include activation of complement to cause inflammation and cell lysis, the opsonization by coating antigen with antibody (e.g., immunoglobulin G, IgG) or complement to enhance the phagocytosis of pathogens through binding to the opsonin receptors of phagocytes, and antibody-dependent cell-mediated cytotoxicity by attaching antibodies to targeted cells to cause the latter's destruction by macrophages, eosinophils, and natural killer (NK) cells. Interestingly, ROS-regulated RHS formed by phagocytes showed the strong viricidal effect on HIV-1 [21,22].

The importance of bats in the evolution of human SARS-CoV-2 that causes the disease COVID-19 has been well documented and indirectly supported by a high degree of similarity with the bat coronavirus genomes. High levels of ROS in bats have been associated with the negative effect on the proof-reading activity of coronavirus RNA polymerases, and it was hypothesized that coronavirus infection in bats is mostly asymptomatic (i.e., bats maintain and disseminate deadly viruses) because

high levels of ROS can indirectly enable the bats to control the levels of viral replication [29]. The bat genes most likely to reflect this phenomenon are those directly related to the first line of antiviral defense—the innate immune system [29].

O₂-dependent degradation in phagocytosis depends on the production of ROS, RHS and RNS, as shown in Figure 1. First, the NADPH oxidase (NOX2) embedded in the phagolysosome membrane is activated to produce O₂^{•-} by O₂ capturing an electron from cytosolic NADPH. H₂O₂ is generated from O₂^{•-} via superoxide dismutases (SOD) or heme(halo)peroxidases (MPO, EPO and LPO); OH[•] is then generated via the Haber-Weiss reaction. Through MPO/EPO/LPO, H₂O₂ activates a halogenating system, which generates hypochlorous acid (HOCl) and kills pathogens [30–34]. The inducible nitric oxide synthases (iNOS) also catalyze the production of NO[•] from L-arginine; NO[•] then reacts with O₂^{•-} to produce a peroxynitrite (ONOO⁻) that forms NO₂ (via reaction with CO₂) [35–37]. The last reaction obviously competes with the SOD-catalyzed scavenging of O₂^{•-}.

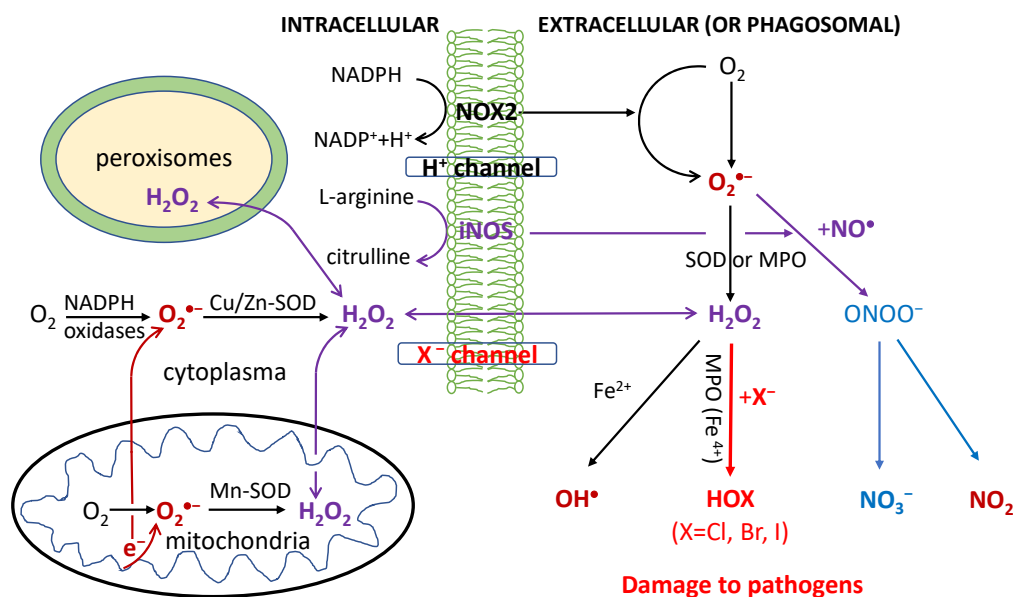


Figure 1. Respiratory burst in the immune defense against pathogens in phagocytosis. Reactive oxygen/halogen/nitrogen species (OH[•]; HOX with X = Cl, Br or I; NO₂) produced within the phagosome cause damage to the DNA/RNA/lipids/proteins of phagocytosed pathogens. The formyl peptide receptors (FPRs) stimulate the activation of the phagocytic NADPH oxidase (NOX2) to form O₂^{•-}, which is rapidly converted to H₂O₂ by the action of cytoplasmic or mitochondrial SOD enzymes. Additionally, H₂O₂ can also be produced extracellularly by the IgG-catalyzed oxidation of water or by the interactions of other receptors such as tumor necrosis factor (TNF) receptors, Toll-like receptors (TLRs) and Nod-like receptors (NLRs) with pathogen-associated ligands. The ROS are also produced by a variety of cell types (nonphagocytic cells) and tissues, catalyzed by six other members of the NOX family including nonphagocytic enzymes NOX1, NOX3, NOX4, NOX5, and the dual oxidases Duox1 and Duox2. The activation of these NOX is stimulated by growth factors, cytokines, and integrins. NOX5 and Duox1 and Duox2 are activated by Ca²⁺ through a cytoplasmic calcium-binding domain. H₂O₂ and NO[•] can diffuse freely across membranes, as indicated by the arrows.

All OH[•], HOCl and ONOO⁻ (NO₂) are strong oxidants believed to damage DNA/RNA, lipids and proteins, and have anti-pathogen effects [30–37]. Particularly HOCl has widely been used as a strong disinfectant; HOBr and HOI at lower levels were also detected in stimulated immune cells [30–34]. Macrophages have weaker antiviral properties than neutrophils and their activation is made by transient respiratory burst, which regulates the inflammatory response by inducing synthesis of cytokines for redox signaling. Due to the high toxicity of ROS/RHS/RNS, damage to host tissues can also occur during inflammation.

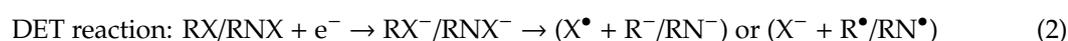
Of particular interest is the role of *endogenous RHS* in the O₂-dependent killing mechanisms of invading pathogens in phagosomes. It is worthy of mention that HOXs (X = Cl, Br) are also important halogen species causing O₃ depletion in the Earth's stratosphere [38,39]. They are derived from solar photolysis [40] or cosmic-ray driven *dissociative-electron-transfer (DET)* reactions [16–19] of halogenated organic molecules, especially CFCs. In radiobiology, there is also a long mystery that the amount of primary ROS produced by IR at clinically relevant radiation doses (2Gy) is ~1000 fold lower than the background (endogenous) ROS level produced by oxidative metabolism of the cell, as first noted by Ward [41]. This leads to the question of how the ROS produced by the few primary ionization events is amplified to account for observed biological effects. The mechanism remains elusive, as recently reviewed by Lehnert [15]. This is a vivid reminder of the hypothesis of significant CFC-induced ozone loss in the Earth's stratosphere by atmospheric scientists in the 1970s, giving birth to the modern ozone depletion theory. It is now well established that there is an amplifying mechanism where a Cl atom catalytically destroys up to 100,000 ozone molecules via halogen reaction cycles [38,39]. Note that during respiratory burst, the increases in O₂ (not NO[•]) consumption were typically observed to be only 2–20 fold among different cells and/or conditions [42]. This, together with the mysterious critical physiological role of H₂O₂, implies that a drastic amplification mechanism is clearly required.

2. Theoretical Studies

2.1. Halogen Cyclic Reactions

Here we hypothesize that (i) the *initial* yields of endogenous ROS/RHS/RNS produced in the phagosome are not sufficient to cause a significant anti-pathogen effect in the immune defense, for which an amplification mechanism is required; (ii) The O₃-depleting-like reaction cycles of RHS take place in the phagosome for immunological defences in cells of humans and all other mammals, via enzymes such as hemeperoxidases or other antioxidant enzymes, instead of solar photons or cosmic rays; (iii) Similar to the formation of polar O₃ hole, numerous reaction cycles of RHS (mainly X[•], XO[•], HOX, OX⁻, X₂; X = Cl or Br or I) play a major role in killing pathogens and immunological defences. These are schematically shown in Figure 2.

In biological systems, the halogenation of organic molecules is catalyzed by enzymes haloperoxidases such as MPO, EPO and LPO in normal physiological processes, which combine the inorganic substrates X⁻ and H₂O₂ to produce RHS. RHS in turn oxidize the hydro-carbon or -nitrogen substrate RH/RNH to synthesize many halogenated organic compounds (RX/RNX):



By reaction (1), many halogenated organic compounds are biosynthesized [32,34,43,44]. It is also well known that halogenated RX/RNX are highly effective for DET reactions that result in anions R⁻/RN⁻/X⁻ or reactive radicals X[•]/OX[•]/R[•]/RN[•], as expressed in reaction (2) [15–19,45–51]. As shown in Table 1, all of these RHS have been found in biological systems especially phagosomes [30–34,43,44,52–54]. One should be cautious with some reaction rate constants listed in Table 1, as they are somewhat outdated. For example, most experiments by nanosecond- or picosecond-resolved radiolysis of aqueous halogenated molecules actually measured the DET with the hydrated electron (e_{aq}⁻) rather than the subpicosecond-lived prehydrated electron (e_{pre}⁻). e_{aq}⁻ is deeply bound at ~3.5 eV and is relatively inert, while e_{pre}⁻ has a small binding energy of 1.0–1.5 eV and is extremely effective for DET with halogenated molecules, as well demonstrated and reviewed previously [18,19,49–51,55,56].

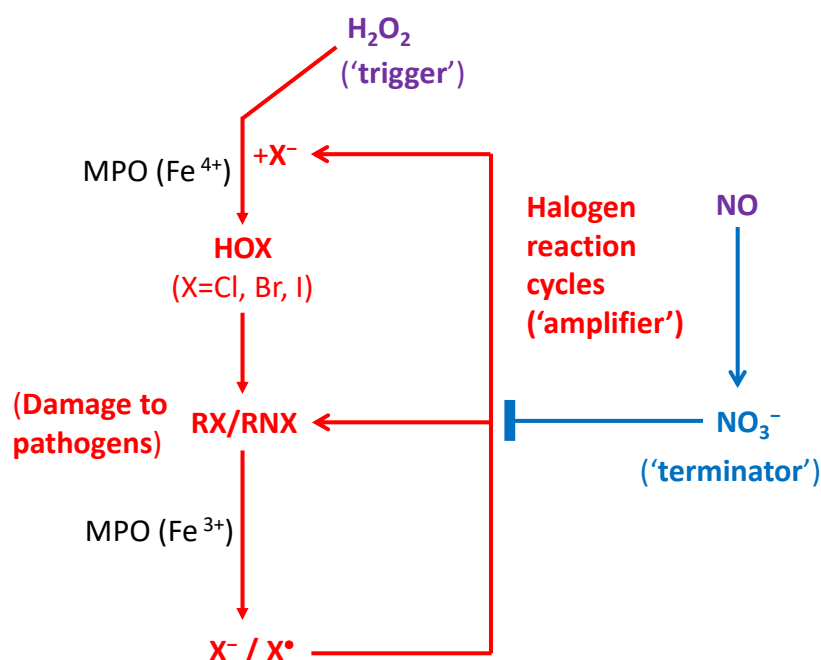


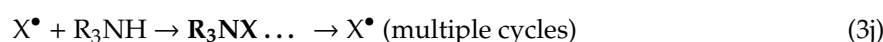
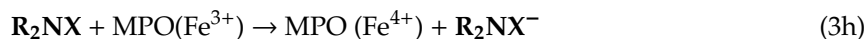
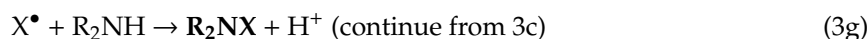
Figure 2. Proposed halogen reaction cycles involved in the immune defense against pathogens and in the inflammatory process. The amplified reactions of reactive halogen species (RHS), including HOX, OX⁻, X₂, X[•] and OX[•] (X = Cl, Br or I), produced by dissociative electron transfer (DET) within the phagosome cause major damage (represented by RX/RNX) to the DNA/RNA/lipids/proteins of phagocytosed pathogens. The immune defence system consists mainly of three components: the H₂O₂ signaling pathway as the trigger, the RHS reaction cycles as the amplifier, and the NO[•] signaling pathway as the terminator. H₂O₂ from other intracellular organelles such as mitochondria and peroxisomes can also diffuse across membranes and promote the anti-pathogen activity.

Table 1. Approximate rate constants (M⁻¹ s⁻¹) for aqueous-phase reactions of some species involved in phagocytosis at pH = 7.0, 288 K.

| Reaction | Products | <i>k</i> (M ⁻¹ s ⁻¹) | Refs |
|---|--|---|---------|
| X ⁻ + H ₂ O ₂ + MPO + H ⁺ | HOX/OX ⁻ /X ₂ + H ₂ O | 2.5 × 10 ⁴ , 1.1 × 10 ⁶ , 7.2 × 10 ⁶ (X = Cl, Br, I) | [31] |
| X ⁻ + H ₂ O ₂ + EPO + H ⁺ | | 3.1 × 10 ³ , 1.9 × 10 ⁷ , 9.3 × 10 ⁷ (X = Cl, Br, I) | |
| Cl ⁻ + OH [•] + H ⁺ | Cl [•] + H ₂ O | 1.5 × 10 ¹⁰ | [39] |
| R ₂ NH + HOX/XO ⁻ | R ₂ NX | 10 ⁷ –10 ⁸ | [44] |
| Cl ₂ + RNH ₂ | RNHX + Cl ⁻ + H ⁺ | (>)10 ⁹ | [44] |
| NH ₂ Cl + e _{aq} ⁻ | Cl ⁻ + NH ₂ | 2.2 × 10 ¹⁰ | [53] |
| R ₂ NCl + e _{aq} ⁻ | Cl ⁻ + R ₂ N [•] | 1.5–1.9 × 10 ¹⁰ | [52,53] |
| RNHCl + e _{aq} ⁻ | Cl ⁻ + RNH [•] | 6.1–9.3 × 10 ⁹ | [52,53] |
| RR'NBr + e _{aq} ⁻ | Br [•] + RR'N ⁻ | 2.9 × 10 ¹⁰ (1.1 × 10 ¹¹) | [52,53] |
| RR'NBr + O ₂ ⁻ | Br [•] + RR'N ⁻ | 2–9 × 10 ⁸ | [52,53] |
| NO ₃ ⁻ + e _{pre} ⁻ | NO ₃ ²⁻ | 1.2 × 10 ¹³ | [55,56] |
| CO ₃ ⁻ + O ₂ ^{•-} | CO ₃ ²⁻ + O ₂ | 4 × 10 ⁸ | [39] |
| NO ₂ + OH [•] | NO ₃ ⁻ + H ⁺ | 1.3 × 10 ⁹ | [39] |

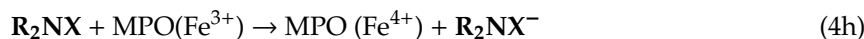
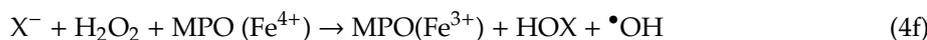
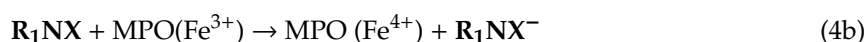
Reactions (1) and (2) lay a solid foundation for halogen cyclic reactions to be presented below. Notably, the standard reduction potentials at pH 7 of all redox couples (Compound I/native enzyme, H₂O) of enzymes MPO/EPO/LPO abundant in phagosomes are relatively small, being 1.09–1.16 V [31,32].

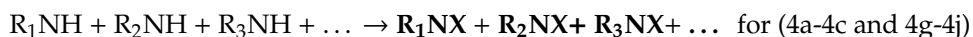
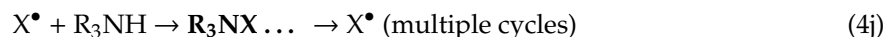
Similarly, the standard reduction potentials at pH 7 of the redox couple (HOX/X⁻, H₂O) for two-electron oxidation of halides are 0.78, 1.13 and 1.28 V for X = I, Br and Cl, respectively [31,32]. Moreover, the exothermic energies for the DET reaction in water of halogenated organic compounds such as RNX is E_A(X) - D(N-X) + E_p [45,46,49–51], where E_A(X) is the electron affinity of a X atom [E_A(Cl) = 3.61 eV; E_A(Br) = 3.36 eV; E_A(I) = 3.06 eV] or the neutral radical RN[•] [E_A(RN) = ~3.46 eV] [57], D(N-X) is the known bond dissociation energy of N-X [D(N-Cl) = 2.08 eV; D(N-Br) = 2.50 eV; D(N-I) = 1.65 eV], and E_p ≈ 1.30 eV [49,50] (1.25–1.50 eV) [58] is the polarization energy of an anion in water. The thus calculated exothermicities for the DET reactions of RNX to form a RN[•] and a X⁻ (or a RN⁻ and a X[•]) are 2.83 (or 2.68), 2.16 (or 2.26) and 2.71 (or 3.11) eV for X = Cl, Br and I, respectively, significantly larger than the reduction energies of the redox couples (Compound I/native enzyme, H₂O) of enzymes MPO/EPO/LPO. For X = Cl, the DET of RNX favors the dissociation pathway to form RN[•] (and X⁻), whereas it preferentially leads to the production of X[•] (and RN⁻) for X = Br and I. These estimates indicate that the catalyzed cyclic reactions of RHS must *effectively* take place and sustain for numerous cycles in phagosomes with those endogenous electron-donating enzymes replacing solar photons or cosmic-ray-produced electrons. This is analogous to the established O₃ depleting cyclic reactions. For example, X[•] and HOX with X = Cl, Br, or I can have the following cyclic reactions (**bold** represents altered targets such as damaged DNA/RNA/proteins in pathogens):



Net: H₂O₂+R₁NH+R₂NH+R₃NH → R₁NX+R₁NR₂NH+R₃NX for (3a-3b and 3d-3f) plus (1) & (2)

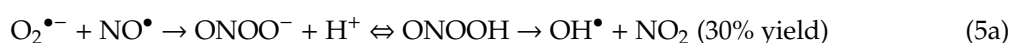
R₁NH+R₂NH+R₃NH + ... → R₁NX+R₂NX+R₃NX+ ... for (3a-3c and 3g-3j)





Note that cycle 1 (reactions 3a–3b and 3d–3f, or reactions 4a–4b and 4d–4f) depends on H_2O_2 , whereas cycle 2 (reactions 3a–3c and 3g–3j, or reactions 4a–4c and 4g–4j) is H_2O_2 independent due to the DET of RN_1X into a X^{\bullet} atom. The net effects of both reaction cycles are the alternations (damages) to at least two biological targets R_1NH and R_2NH with no halogen consumption. Similar reaction cycles can occur for other RHS such as XO^{\bullet} and X_2 . They are most effective (i.e., cycle 2 occurs), if the X^{\bullet} atom is yielded, which was indeed observed for radiolysis of N-bromoimides but not for N-chloroimides [52,53]. Cycle 2 will be more significant with the formation of X_2 in reaction (1) (as $X_2 + e^- \rightarrow X^{\bullet} + X^-$ readily), and therefore will become dominant as the halogen level reaches above a threshold. Indeed, HOX was also observed to be in equilibrium with X_2 or BrCl in the MPO- H_2O_2 -halide system under acidic conditions in the presence of excess X^- , as in phagosomes [31,32,43,44]. Cycles 1 and 2 are expected to continue for numerous cycles before they are terminated. Note that the peroxidase cycle [30–34] in catalyzing the reaction ($X^- + H_2O_2 \rightleftharpoons HOX + H_2O$), and the radical chain [52,53] in radiolysis of N-halogenated species ($R^{\bullet} + Br_2 \rightarrow RBr + Br^{\bullet}$; $Br^{\bullet} + RH \rightarrow H^{\bullet} + Br^- + R^{\bullet}$. Net: $Br_2 + RH \rightarrow RBr + Br^- + H^{\bullet}$) as originally suggested by Goldfinger et al. [59], have been proposed previously to enhance the reaction efficiency, but each of those reaction cycles occurs at the consumption of a halogen species. They are therefore distinct from the O_3 -depleting-like DET-based halogen reaction cycles proposed here that have no cost of halogens (acting as “catalysts”). A question then arises: how would the halogen reaction cycles be terminated?

In atmospheric photochemistry of ozone loss, RHS is removed from the catalytic cycles once the reaction ends with HX or $XONO_2$ (“inactive reservoirs”) [38,39]. In the phagosome (cell), however, this would not be the case as aqueous HCl can readily react with OH^{\bullet}/HOX to form X^{\bullet}/X_2 and the hydrolysis of $XONO_2$ will quickly occur to form XO^{\bullet} and NO_2 . It is worth noting that the above proposed cyclic reactions are essentially enzyme-driven electron-transfer reactions. Peroxynitrite has a half life of 1.9 s at pH 7.4 and its decomposition leads to a major product nitrate (NO_3^-) and a minor product of CO_3^- or NO_2 with/without reaction with CO_2 [35,36]:



Since the redox potential of NO_2 is close to that OH^{\bullet} , $ONOO^-$ is believed to act as an OH^{\bullet} -like oxidizing species in causing damaging effects [35,36]. Notably, NO_3^- is known to be an extremely effective scavenger for weakly-bound electrons (NO_3 has an electron affinity of 3.94 eV, larger than any halogen) [50,55,56], with the measured reaction rate constant of as large as $1.2(\pm 0.5) \times 10^{13} \text{ M}^{-1}\text{s}^{-1}$ [56]. Reaction of CO_3^- with electrons or $O_2^{\bullet-}$ is also expected (see Table 1). Thus, the halogen reaction cycles would be terminated if there is a significant amount of NO_3^- or CO_3^- (mainly NO_3^-) in the phagosome. Remarkably, the reduction or removal of nitrogen species (HNO_3 as the ultimate product) is a critical requirement for the formation of the ozone hole (significant ozone loss) in the polar stratosphere [38,39].

It follows that our proposed immune defence system fighting against pathogens is composed of three components: the H_2O_2 signaling pathway is the activator (“trigger”), the RHS reaction cycles the accelerator (“amplifier”), and the NO^{\bullet} signaling pathway (NO_3^-) the deactivator (“terminator”) of RHS reactions, as shown in Figure 2. The delicate balance between the two regulations, by H_2O_2

and NO^\bullet , is responsible for immunity that allows multicellular organisms to have adequate biological defenses to fight infection, disease, or other unwanted biological invasion, while having adequate tolerance to avoid allergy and autoimmune diseases/disorders. Note that as stable and small neutral signaling molecules that can diffuse easily across the membrane, both H_2O_2 and NO^\bullet from other cellular organelles such as peroxisomes and mitochondria can also be involved in the defense system [60].

2.2. Halogen Cyclic Reaction Rates

It is striking to find the close similarity between the negative ion chemistry in the undisturbed stratosphere and troposphere of the Earth and that in phagosomes of the cell, as shown in Figure 3. Both are quite similar, involving identical species of $\text{O}_2^{\bullet-}$, CO_2 , NO , NO_2 , and ONOO^- [19,61,62], except that O_3 is far more abundant in the stratosphere though its presence in phagosomes was also arguably observed [32]. For negative ion chemistry in the atmosphere, the primary ions are quickly converted into $\text{CO}_3^-(\text{H}_2\text{O})_n$ ions on the order of 10^{-3} s by a series of reactions with O_2 , CO_2 , O_3 and H_2O [61,62]. In the stratosphere, the $\text{CO}_3^-(\text{H}_2\text{O})_n$ ions are converted relatively slowly into the more stable ions $\text{NO}_3^-(\text{H}_2\text{O})_n$ or $\text{NO}_3^-(\text{HNO}_3)_m(\text{H}_2\text{O})_n$ on the order of 1 s by reaction with the trace gases NO , NO_2 , HNO_3 , and N_2O_5 [61,62]. For altitudes below 30 km, the hydrated NO_3^- ions are the dominant and *terminal* species. The positive-ion chemistry is even simpler and the cluster ions $\text{H}_3\text{O}^+(\text{H}_2\text{O})_n$ ($n = 3-6$) are the sole primary ions since their formation is also rapid (10^{-3} s). This is much shorter than the (positive) ion- (negative) ion recombination lifetime (i.e., the residence time of ions) of approximately 100–1000 s in the atmosphere [62].

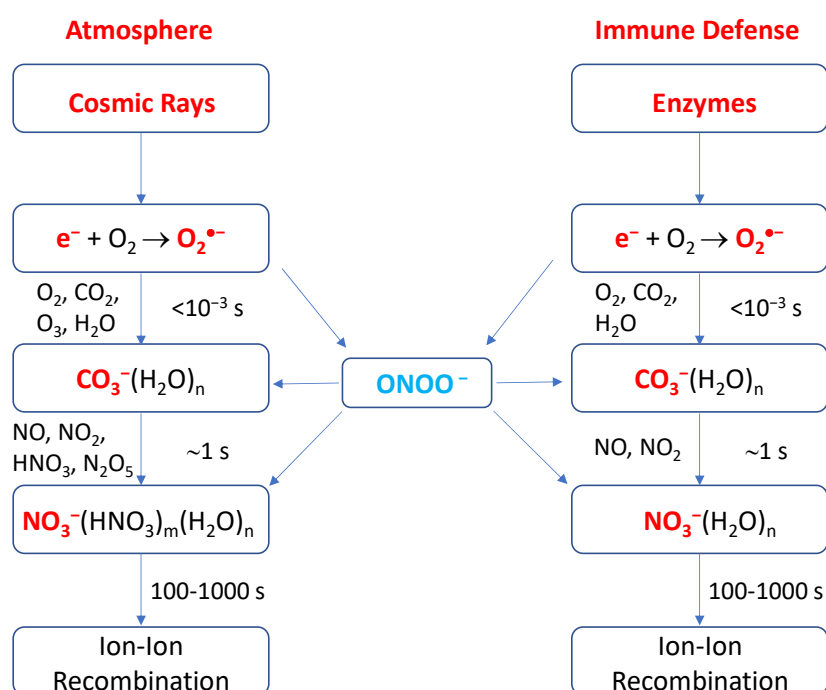


Figure 3. Schematic representations of the negative ion chemistry in the undisturbed stratosphere and troposphere of the Earth [61,62] and in the phagolysosome in the innate immune defense system in humans.

Looking into the rate constants in Table 1 and reactant abundances of all the cyclic reactions (1–5), we can see that reaction (1) or (3f) or (4f) is the rate-determining step; that is, the haloperoxidase catalyzed converting reaction of X^- and H_2O_2 into HOX is the rate-limiting reaction. We further notice that H_2O_2 is stable, while the lifetime of negative ions including $\text{Cl}^-/\text{Br}^-/\text{I}^-$ and NO_3^- is controlled by the recombination time with the abundant hydronium ions $\text{H}_3\text{O}^+(\text{H}_2\text{O})_n$ (protons) in the acidic phagolysosome, which are long-lived, in contrast to hydronium in neutral solutions. It was indeed

observed that the increase in IR-stimulated ROS/RNS generation persisted for 2–5 min post-irradiation in most cell lines and for ~15 min after irradiation in some cell lines [63]. Thus, the reaction period of RHS in the phagolysosome is approximately 100–1000 s, identical to that in the lower atmosphere. Given the Cl^- and Br^- concentrations in phagocytes are 120 mM (median) and 60 μM (median) [54] and the rate constants of 2.6×10^4 – $3.9 \times 10^6 \text{ M}^{-1} \text{ s}^{-1}$ and 3.0×10^7 – $1.1 \times 10^8 \text{ M}^{-1} \text{ s}^{-1}$ for the converting reactions with H_2O_2 at pH 5.0 respectively [64,65], we calculate that the overall Cl and Br cyclic reactions occur with respective rates of approximately 3120 – $4.68 \times 10^5 \text{ s}^{-1}$ and 1800 – 6600 s^{-1} . These give rise to *at least* 3.1×10^5 – 4.7×10^7 and 1.8×10^5 – 6.6×10^5 reaction cycles during the lifetime ($\geq 100 \text{ s}$) of Cl^- and Br^- in the phagolysosome respectively. These estimated values are fairly close to the ozone depleting reaction cycles in the atmosphere [38]. These appear quite surprising, but they are actually mainly determined by the levels of Cl^- and Br^- and the ion residence time. The latter is governed by the recombination with $\text{H}_3\text{O}^+(\text{H}_2\text{O})_n$ [61,62], resulting in the apparently identical ion lifetime in both the stratosphere and the phagolysosome.

It must be noted that although the proposal of halogen reaction cycles in phagocytosis appears striking and novel, each of the reactions (1–5) is very well-established in the literature [15–19,43–51]. Given the abundances and low reduction potentials [31,32] of endogenous haloperoxidases (MPO/EPO/LPO) in phagosomes and the high resemblance [19,61,62] of the negative ion chemistry in phagosome to that in the atmosphere, there is every reason to deduce that the reaction cycles can be repeated thousands of times and amplify the RHS pathogen-killing (defense) effects by $\sim 10^5$ fold, analogous to the cyclic ozone-depleting reactions [38]. For the latter, RHS is known to be far more efficient than OH and NO at catalyzing the destruction of ozone, and among RHS, Br or I is much more efficient than Cl at catalyzing the cyclic reactions [18,19,38,39,45,46,49,50].

2.3. Significance of Halogen Cyclic Reactions

This proposed mechanism has multifold significance:

- (1) The H_2O_2 -initiated halogen cyclic reactions should greatly amplify the pathogen-killing effects of RHS in phagocytosis for innate and adaptive immune defenses. The proposed mechanism might lead to discoveries of highly effective antiviral drugs for effective treatment of various viruses such as HIV and COVID-19.
- (2) It also provides a long-sought amplification mechanism for reactive radicals produced by IR to generate the clinically required radiobiological effects in human body, as compared with background ROS.
- (3) It reveals that H_2O_2 as a signaling molecule plays the key protective (pathogen-killing) role in immunological defenses in many organisms from plants and animals to humans.
- (4) It also unravels the crucial physiological role of H_2O_2 to account for the observed critical effect of enzymes SOD [8–15]. Once the SOD was impaired, the dysfunction of H_2O_2 as the protective molecule in the immune system resulted in and the animals died quickly.

2.4. Implications for the Pathology of COVID-19

If people infected by an acute pathogen like SARS-CoV-2 that causes COVID-19 show mild and moderate symptoms and receive no or improper treatment, they might rapidly develop into severe cases of extreme respiratory burst. In the latter case, the halogen cyclic killing reactions may result in dysfunctions or disorders of closely interacting and communicating cell organelles, such as peroxisomes, mitochondria and lysosomes, and even severe damage to the host cells and tissues during autoimmune (over inflammation), by analogy with the severe springtime Antarctic ozone hole. The over toxicity caused by amplified RHS reactions is expected to result in unrepairable damage or mutations to cellular components, and the signaling pathways of H_2O_2 and NO^\bullet may be impaired as well. Disorders in these organelles can cause serious damage to multiple organs such as lung, heart,

liver, kidney and nervous systems, and respiratory failure, septic shock, multi-organ failure or even deaths. The best treatment should be in early or moderate stage or prevention.

3. Halogenated Aromatic Drugs as Repurposed Drugs

Given our new understanding of the pathology of invading pathogens described above, we now discuss potential treatment of the severe virus COVID-19. Exogenous halogenated aromatic ring compounds as neutral small molecules that can freely diffuse across membrane will be potent anti-pathogen agents. Here we present a new molecular mechanism of action (MOA) of a class of halogenated aromatic drugs such as chloroquine and hydroxychloroquine (HCQ), which have been a current focus for experimental treatment of COVID-19 [66–68] and more potent di-amino, di-halogen aromatic ring molecules [termed *fentomedicine* compounds, FMDs], which have exhibited excellent targeted chemotherapy of multiple cancers [69–71]. These drugs or candidates are promising for effective treatments of COVID-19, cancer and other diseases.

For the MOA of HCQ and chloroquine, the readers are referred to a recent review [72]. As noted by the reviewers, most of the MOAs to explain the therapeutic and/or adverse effects were hypothesized based on in-vitro studies, and the link between the proposed MOAs and the clinical efficacy and in vivo safety is yet to establish. The proposed molecular MOA of HCQ during autoimmunity include the following processes. Pharmacodynamic studies showed that these antimalarial drugs are lipophilic weak bases, easily cross plasma membranes, and preferentially accumulate in lysosomes, causing increases in the pH of lysosomes from 4 to 6 [73]. Elevation in pH causes inhibition of lysosomal activity including diminished proteolysis effect [74], decreased intracellular processing, glycosylation and secretion of proteins with many consequences [75]. These effects are believed to cause a decreased immune cell functioning such as chemotaxis, phagocytosis and $O_2^{\bullet-}$ production by neutrophils [76].

Another proposed MOA was that HCQ inhibits Toll-like receptor (TLR) signaling. This speculation might be traced back to a review [77]. The authors reviewed potent antiviral and antitumor properties of several imidazoquinolines as nucleic acid analogs, for which TLR7 was suggested to sense viral infection. Also, their unpublished data showed that two other immunomodulators, loxoribine and bropirimine, also activated immune cells through TLR7. Bropirimine (2-amin-5-bromo-6-phenyl-4(3)-pyrimidinone) is an immunomodulator that induces production of cytokines including IFN- α . There has been interest in searching TLR-activating agents for clinical use. Takeda et al. [77] predicted that new therapies utilizing the TLR-mediated innate immune activation would be developed to treat several disorders such as infection, cancer and allergy. Due to some structural similarity to these imidazoquinolines, there have been speculations that TLR7 and TLR9 receptors are involved in the MOA of HCQ.

Overall, available data suggest that HCQ and chloroquine impair or inhibit lysosomal and phagolysosome functions and subsequently immune activation. There are current efforts to identify exact molecular targets of HCQ within the lysosome, but convincing results and the identification of other molecular targets within the lysosomes have not yet reached. The precise molecular mechanisms of anti-pathogen effects these drugs remain essentially unknown [72].

3.1. New Molecular Mechanism of Action (MOA) of Halogenated Aromatic Drugs

Here we propose a new molecular MOA of halogen-containing aromatic ring drugs represented by AXs, including HCQ and chloroquine, and a family of FMD halogenated compounds [69–71]. Here A is a quine ring system and X = Cl for HCQ and chloroquine, whereas A is an aromatic ring coupled to two NH_2 groups at ortho positions [$A = B(NH_2)_2$] and X = Cl_n or Br_n or I_n with $n = 1,2$ for FMD compounds such as 4,5-dichloro/dibromo/diiodo-1,2-diaminobenzene and 4(5)-chloro/bromo/iodo-1,2-diaminobenzene [69,70]. We propose that these molecules are highly effective for DET reactions and their action is quite similar to the formation of endogenous RHS in the phagosome. It has been long known that the DET reactions of halogenated aromatic organic molecules AXs with weakly-bound electrons in water are highly effective [18,19,45–51]. The exothermic energy for the DET reaction in water is $E_A(X) - D(A-X) + E_p$ [18,19,45–51], where $E_A(X)$ and E_p are

defined earlier and $D(A-X)$ is the known bond dissociation energy of $C-X$ [$D(C-Cl) = 3.43$ eV; $D(C-Br) = 2.81$ eV; $D(C-I) = 2.50$ eV]. The thus estimated exothermic energies for the DET reactions of AXs to form A^\bullet and X^- (or A^- and X^\bullet) are 1.48 (or 1.37), 1.85 (or 1.99) and 1.86 (or 2.3) eV, respectively for $X = Cl, Br$ and I . These exothermicities are significantly larger than the reduction energies (1.09–1.16 eV) [31,32] of the redox couples (Compound I/native enzyme, H_2O) of enzymes MPO, EPO and LPO, indicating that the DET reactions of AXs must effectively take place in phagosomes, as shown in Figure 4. Again, the formation of Br^\bullet or I^\bullet atom (and A^-) is the favorable DET pathway for brominated and iodized AXs, in contrast to that for the DET of chlorinated AXs that favors the formation of Cl^- (and A^\bullet).

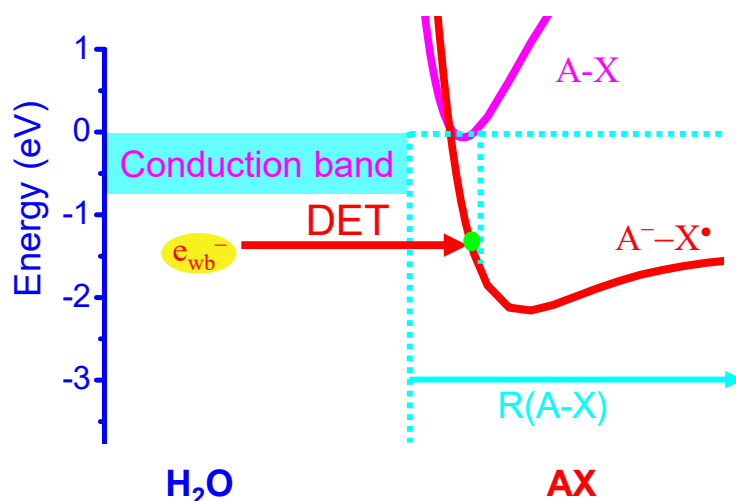
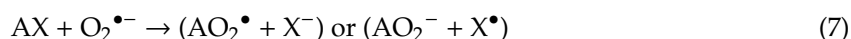


Figure 4. Schematic diagram for the dissociative electron transfer (DET) reaction [18,19,49,50] of a halogenated aromatic ring molecule AX with a weakly-bound electron (e_{wb}^-) in phagosomes, where e_{wb}^- is readily donated from a variety of enzymes or antioxidants or $O_2^{\bullet-}$. For HCQ and chloroquine, A is a quine ring system and $X = Cl$, whereas A is an aromatic ring coupled to two NH_2 groups at ortho positions [$A = B(NH_2)_2$] and $X = Cl_n$ or Br_n or I_n with $n = 1,2$ for FMD compounds) [69,70].

Thus, similar to the DET reactions of endogenous halogenated organic compounds, effective DET reactions of AXs must occur with the enzymes such as MPO/EPO/LPO/SOD or NADPH which are weakly-bound electron donors:



In addition, DET reactions of AXs with $O_2^{\bullet-}$ can also occur with or without the involvement of enzymes in the phagolysosome [78]:



Correspondingly, the halogen atom radicals X^\bullet have particularly effective reaction cycle 2 to amplify the biological effects. The formed reactive radical AO_2^\bullet can also directly cause damaging effects, e.g., by hydrogen abstraction from DNA/RNA, lipids or proteins, while X^- like endogenous halogen ions can be converted into HOX , OX^\bullet , X^\bullet and X_2 via the enzymes MPO/EPO/LPO. Like endogenous $HOCl/HOBr/HOI$, these exogenous RHS will have the amplifying cyclic reactions and cause significant anti-pathogen effects for immunological defence.

3.2. Potential New Therapeutics

As observed for HCQ, these neutral small-molecule AXs including FMD compounds can easily cross plasma membranes to accumulate in lysosomes. We propose that the MOA of these halogenated drugs or candidates should be due to the *enhanced* (rather than inhibited) pathogen-killing effect induced

by the reaction cycles of RHS derived from the DET of the compounds. Indeed, the DET reaction of HCQ will lead to an increase in the Cl^- yield, equivalent to a rise in pH in lysosomes, consistent with the observation for HCQ. When there are invading pathogens in early or intermediate stages, pathogens are effectively killed in the formed phagolysosomes with excess RHS before autoimmune occurs. Since the DET reaction efficiencies are expected to increase in the order of $\text{Cl} < \text{Br} < \text{I}$ for X in AXs [45,46,49,50], as we already observed for halopyrimidines (CldU, BrdU, IdU) [49,50], and more critically the DET reactions of Br- and I-containing aromatic ring molecules preferably produce Br^\bullet or I^\bullet atoms to activate cycle 2 reactions, the in-vivo therapeutic efficacy should increase in the order of $\text{ACl}_n \ll \text{ABr}_n < \text{AI}_n$ ($n = 1,2$).

As for anti-cancer activity of AXs, similar RHS are expected to be generated and to cause apoptosis and cancer cell killing. Moreover, since both H_2O_2 and NO are neutral small signaling molecules that can diffuse freely across the membrane and have high mobility, similar reaction cycles of RHS are expected to take place in other intracellular organelles such as mitochondria and peroxisomes which are electron (antioxidant)-rich. Indeed, recent in-vitro and in-vivo experimental results of multiple cancers have confirmed that the anti-tumor efficacies of the FMD compounds increases in the order of $\text{ACl}_2 \ll \text{ABr}_2 < \text{AI}_2$ [69,70]. Moreover, our unpublished data [79] by direct, real-time femtosecond laser spectroscopic measurements have confirmed the highly effective DET reactions of the FMD compounds.

Notably, the FMD compounds distinguish themselves from other drugs such as HCQ and chloroquine, bropirimine, BrdU and IdU, not only by yielding highly reactive Br^\bullet or I^\bullet atoms to initiate the powerful H_2O_2 -independent reaction cycle but by a unique structural characteristic that contains two NH_2 groups attached to the ring system at ortho positions. This idea is based on a previous finding by Lu and Madey [16,47] that the presence of ammonia can cause giant enhancements in the DET reaction efficacies of CFCs adsorbed on ice surfaces by up to 30,000 times, which was subsequently confirmed by Stähler et al. [51]. Although in vivo DET efficiencies may not be enhanced to this extent, there is every reason to expect that the DET reactions of the FMD compounds should be at least 10 times more effective than any other halogenated organic molecules without the two neighboring NH_2 groups in their structures. This was indeed observed by comparing the DET reactions of FMDs with BrdU and IdU [79]. BrdU is very similar to bropirimine in structure [77]. Thus, we predict that the in-vivo anti-pathogen effectiveness of FMD compounds with proper formulations will be at least 10 times higher than that of any of HCQ, chloroquine, bropirimine, BrdU and IdU.

Also of particular interest is the finding that in treated normal cells, a FMD compound at 100 μM caused an increase of about 40% of the reduced glutathione (GSH) level, which is an endogenous protective antioxidant [15,32], whereas the GSH level in human cervical (ME-180) cancer cells significantly dropped upon treated by the FMD and decreased to ~35% at 100 μM FMD [69]. This marked selective depletion of the GSH was consistent with the proposed preferential DET reaction to activate in cancer cells and with the observed selective cytotoxic effects of FMDs in vitro and in vivo [69–71]. These results showed that FMDs even have a protective effect on normal cells while killing abnormal cells and can be used as targeted chemotherapeutic agents [69,70].

Although no tests on antiviral activity of FMD compounds have been performed, our new studies on animal cancer models have shown that FMDs such as 4,5-dibromo-1,2-diaminobenzene and 4,5-diiodo-1,2-diaminobenzene at doses of ≤ 35 mg/kg (i.p) showed a superior efficacy in anti-cancer activity (leading to significant tumor shrinkage) to the clinical drugs such as cisplatin and gemcitabine at doses that showed significant toxic side effects. In contrast, the maximum tolerated dose (MTD) of 4,5-dibromo-1,2-diaminobenzene was measured to be 220 ± 20 mg/kg (i.p), and no significant multiple dose toxicity in blood, liver, kidney, gut and spleen for 90 mg/kg/week for 4 weeks in mice (i.v) were observed. The oral MTD, which is usually at least 5 times higher, may be over 1000 mg/kg. These results indicate that FMDs are essentially non-toxic but highly effective chemotherapeutic agents at used doses that can preferentially kill abnormal cells. It is therefore useful for natural targeted chemotherapy of cancer and other diseases, which potentially include viral infections and autoimmune

disorders. By contrast, due to the increased risk of developing retinopathy during treatment with HCQ, the current ophthalmology guidelines recommend a maximal daily dose of 5.0 mg/kg (actual body weight) per day for HCQ, while in cancer studies, high HCQ doses up to 1200 mg (17–18 mg/kg) daily was prescribed [72,80]. Given these data, FMD compounds are estimated to have a clinical safe dose at least 10 times higher than HCQ in humans. Thus, FMDs at a wide non-toxic dose range have high potential to outperform existing drugs such as chloroquine and HCQ that have known toxic side effects.

Caly et al. [81] reported that the FDA-approved ivermectin, a protease inhibitor for the treatment of parasitic infections and for the replication of HIV and Dengue viruses, inhibits replication of SARS-CoV-2 in vitro, making it a possible candidate for COVID-19 drug repurposing research. Interestingly, pharmacological studies showed that the drug binds to glutamate-gated chloride channels (GluCl_s, present in neurons and myocytes) in the membranes of invertebrate nerve and muscle cells, causing increased permeability to Cl⁻ ions, resulting in cellular hyper-polarization, followed by paralysis and death. The pathology proposed in this paper can well explain the MOA of this drug: the increased Cl⁻ permeability will elevate the Cl⁻ level and the associated RHS cyclic reactions to enhance the pathogen-killing effects.

Also, emerging studies to understand the pathogenesis of SARS-CoV-2 have just been published [82,83]. By analyzing human, non-human primate, and mouse single-cell RNA-sequencing (scRNA-seq) datasets and identifying ACE2 and TMPRSS2 co-expressing cells in lung type II pneumocytes, ileal absorptive enterocytes, and nasal goblet secretory cells, Ziegler et al. [82] showed that ACE2 is *enhanced* in human nasal epithelia and lung tissue by interferon and influenza but not upregulated in mice. They proposed that SARS-CoV-2 could exploit species-specific interferon-driven upregulation of ACE2, a tissue-protective mediator during lung injury, to enhance infection. In contrast, by analysis of the transcriptional response to SARS-CoV-2 compared with other respiratory viruses, Blanco-Melo et al. [83] found that cell and animal models of SARS-CoV-2 infections, as well as transcriptional and serum profiling of COVID-19 patients, consistently showed a unique and inappropriate inflammatory response, which was defined by low levels of Type I and III interferons juxtaposed to elevated chemokines and high expression of IL-6. The latter study therefore suggested that the deficit in innate antiviral defenses coupled with abundant inflammatory cytokine production is the defining and driving feature of COVID-19. It seems that a consistent pathogenesis of COVID-19 has not yet emerged. Further studies are obviously needed.

4. Conclusions

Provided with the pathology of infection and molecular MOA of drugs proposed in this paper, drugs (candidates) like FMDs will enhance rather than inhibit the endogenous pathogen-killing effect in the immune system in humans. These halogenated aromatic drugs may be used for experimental treatment of COVID-19, especially for preventive, mild and moderate stages, and probably treatment of developed chronic conditions. In these applications, the halogen compounds should provide strong pathogen-killing effects. During autoimmune disorders, however, precaution should be taken if these drugs are to be used, because they will produce an excess number of exogenous RHS, much larger than that of endogenous RHS. In the latter case, using a NO (iNOS) inducer to enhance the production of the electron killer (NO₃⁻/CO₃⁻) neutralizing RHS might be helpful to the patients. This paper provides a plausible molecular mechanism that might help with clinical practice of the drugs. It may improve the clinical efficacy, control the toxicity within a tolerated range, and suggest the optimal timing/sequential administration or possible combination therapy. This might meet the current medical challenges faced in this global pandemic and save many lives across the globe. Furthermore, this research also reveals that H₂O₂ is a necessary signaling molecules (angel) in the defense system fighting against pathogens and maintaining normal physiological functioning and signaling and its dysfunction can cause many diseases of organisms ranging from plants to humans. The role of phagocytosis in both innate and adaptive immune defenses is probably underestimated under the current context of

immunology and virology. New mechanistic insights into immune defense might lead to a discovery and development of more potent and/or targeted drugs for treatment of many diseases or conditions such as viral infections such as HIV and SARS-COV-2 (COVID-19), aging and cancer.

Funding: This research was supported in part by the Canadian Institutes of Health Research (a grant to Q.B.L, # 51771-10127) and Natural Science and Engineering Research Council of Canada (NSERC, a grant to Q.B.L, # 50503-10603). No other funding sources have been provided in the writing of this manuscript or the decision to submit it for publication.

Acknowledgments: Correspondence and requests for materials should be addressed to Q.B.L. (qblu@uwaterloo.ca).

Conflicts of Interest: The author declares that there were issued patents or submitted patent applications associated with the data reported in this manuscript.

References

1. Rhee, S.G. CELL SIGNALING: H₂O₂, a Necessary Evil for Cell Signaling. *Science* **2006**, *312*, 1882–1883. [[CrossRef](#)]
2. Veal, E.A.; Day, A.M.; Morgan, B.A. Hydrogen peroxide sensing and signaling. *Mol. Cell* **2007**, *26*, 1–14. [[CrossRef](#)] [[PubMed](#)]
3. Watson, J.D. Type 2 diabetes as a redox disease. *Lancet* **2014**, *383*, 841–843. [[CrossRef](#)]
4. Lambeth, J.D.; Neish, A.S. Nox Enzymes and New Thinking on Reactive Oxygen: A Double-Edged Sword Revisited. *Annu. Rev. Pathol. Mech. Dis.* **2014**, *9*, 119–145. [[CrossRef](#)] [[PubMed](#)]
5. Sies, H. Hydrogen peroxide as a central redox signaling molecule in physiological oxidative stress: Oxidative eustress. *Redox. Biol.* **2017**, *11*, 613–619. [[CrossRef](#)] [[PubMed](#)]
6. Torres, M.A.; Jones, J.D.G.; Dang, J.L. Reactive Oxygen Species Signaling in Response to Pathogens. *Plant Physiol.* **2006**, *141*, 373–378. [[CrossRef](#)] [[PubMed](#)]
7. McCord, J.M.; Fridovich, I. Superoxide dismutase. An enzymic function for erythrocyte superoxide (heine). *J. Biol. Chem.* **1969**, *244*, 6049–6055.
8. Li, Y.; Huang, T.T.; Carlson, E.J.; Melov, S.; Ursell, P.C.; Olson, J.L.; Noble, L.J.; Yoshimura, M.P.; Berger, C.; Chan, P.H.; et al. Dilated cardiomyopathy and neonatal lethality in mutant mice lacking manganese superoxide dismutase. *Nat. Genet.* **1995**, *11*, 376–381. [[CrossRef](#)]
9. Elchuri, S.; Oberley, T.D.; Qi, W.; Eisenstein, R.S.; Jackson, R.L.; Van Remmen, H.; Epstein, C.J.; Huang, T.-T. Cu/Zn-SOD deficiency leads to persistent and widespread oxidative damage and hepatocarcinogenesis later in life. *Oncogene* **2005**, *24*, 367–380. [[CrossRef](#)]
10. Muller, F.L.; Song, W.; Liu, Y.; Chaudhuri, A.; Pieke-Dahl, S.; Strong, R.; Huang, T.-T.; Epstein, C.J.; Roberts, L.J., 2nd; Csete, M.; et al. Absence of Cu/Zn superoxide dismutase leads to elevated oxidative stress and acceleration of age-dependent skeletal muscle atrophy. *Free. Rad. Bio. Med.* **2006**, *40*, 1993–2004. [[CrossRef](#)]
11. Williams, M.D.; van Remmen, H.; Conrad, C.C.; Huang, T.T.; Epstein, C.J.; Richardson, A. Increased oxidative damage is correlated to altered mitochondrial function in heterozygous manganese superoxide dismutase knockout mice. *J. Biol. Chem.* **1998**, *273*, 28510–28515. [[CrossRef](#)] [[PubMed](#)]
12. Oberley, L.W.; Lindgren, A.L.; Baker, S.A.; Stevens, R.H. Superoxide ion as the cause of the oxygen effect. *Radiat. Res.* **1976**, *68*, 320–328. [[CrossRef](#)] [[PubMed](#)]
13. Petkau, A.; Chelack, W.S.; Pleskach, S.D. Protection of post irradiated mice by superoxide dismutase. *Int. J. Radiat. Biol.* **1976**, *29*, 297–299. [[CrossRef](#)] [[PubMed](#)]
14. Spitz, D.R.; Azzam, E.I.; Li, J.L.; Gius, D. Metabolic oxidation/reduction reactions and cellular responses to ionizing radiation: A unifying concept in stress response biology. *Cancer Metastasis Rev.* **2004**, *23*, 311–322. [[CrossRef](#)]
15. Lehnert, S. *Biomolecular Action of Ionizing Radiation*; CRC Press: Boca Raton, FL, USA, 2008; pp. 97–120.
16. Lu, Q.B.; Madey, T.E. Giant enhancement of electron-induced dissociation of chlorofluorocarbons coadsorbed with water or ammonia ices: Implications for the atmospheric ozone depletion. *J. Chem. Phys.* **1999**, *111*, 2861–2864. [[CrossRef](#)]
17. Lu, Q.B.; Sanche, L. Effects of Cosmic Rays on Atmospheric Chlorofluorocarbon Dissociation and Ozone Depletion. *Phys. Rev. Lett.* **2001**, *87*, 078501. [[CrossRef](#)]

18. Lu, Q.B. Cosmic-Ray-Driven Electron-Induced Reactions of Halogenated Molecules Adsorbed on Ice Surfaces: Implications for Atmospheric Ozone Depletion and Global Climate Change. *Phys. Rep.* **2010**, *487*, 141–167. [[CrossRef](#)]
19. Lu, Q.B. *New Theories and Predictions of the Ozone Hole and Climate Change*; World Scientific: Hackensack, NJ, USA, 2015; Chapters 1, 4 & 5.
20. Peterhans, E.; Grob, M.; Burge, T.H.; Zanoni, R. Virus-Induced Formation of Reactive Oxygen Intermediates in Phagocytic Cells. *Free Rad. Res. Comms.* **1987**, *3*, 39–46. [[CrossRef](#)]
21. Chase, M.J.; Klebanoff, S.J. Viricidal effect of stimulated human mononuclear phagocytes on human immunodeficiency virus type 1. *Proc. Natl. Acad. Sci. USA* **1992**, *89*, 5582–5585. [[CrossRef](#)]
22. Klebanoff, S.J.; Coombs, R.W. Viricidal effect of polymorphonuclear leukocytes on HIV-1: Role of the myeloperoxidase system. *J. Clin. Investig.* **1992**, *89*, 2014–2017. [[CrossRef](#)]
23. Kramer, M.; Schulte, B.M.; Toonen, L.W.J.; Barral, P.M.; Fisher, P.B.; Lanke, K.H.W.; Galama, J.M.D.; van Kuppeveld, F.J.M.; Adema, G.J. Phagocytosis of Picornavirus-Infected Cells Induces an RNA-Dependent Antiviral State in Human Dendritic Cells. *J. Virol.* **2008**, *82*, 2930–2937. [[CrossRef](#)] [[PubMed](#)]
24. Vangeti, S.; Yu, M.; Smed-Sørensen, A. Respiratory Mononuclear Phagocytes in Human Influenza A Virus Infection: Their Role in Immune Protection and As Targets of the Virus. *Front. Immunol.* **2018**, *9*, 1521. [[CrossRef](#)] [[PubMed](#)]
25. Rogers, K.J.; Maury, W. The role of mononuclear phagocytes in Ebola virus infection. *J. Leukoc. Biol.* **2018**, *104*, 717–727. [[CrossRef](#)] [[PubMed](#)]
26. Van Strijp, J.A.G.; Kok, P.M.; Kessel, V.; van der Tol, M.E.; Verhoef, J. Complement-mediated Phagocytosis of Herpes Simplex Virus by Granulocytes Binding or Ingestion. *J. Clin. Investig.* **1989**, *84*, 107–112. [[CrossRef](#)]
27. Powell, L.R.R.; Fox, A.; Itri, V.; Zolla-Pazner, S. Primary Human Neutrophils Exhibit a Unique HIV-Directed Antibody-Dependent Phagocytosis Profile. *J. Innate Immun.* **2019**, *11*, 181–190. [[CrossRef](#)]
28. Tay, M.Z.; Wiehe, K.; Pollara, J. Antibody-Dependent Cellular Phagocytosis in Antiviral Immune Responses. *Front. Immunol.* **2019**, *10*, 332. [[CrossRef](#)]
29. Zhang, G.; Cowled, C.; Shi, Z.; Huang, Z.; Bishop-Lilly, K.A.; Fang, X.; Wynne, J.W.; Xiong, Z.; Baker, M.L.; Zhao, W.; et al. Comparative Analysis of Bat Genomes Provides Insight into the Evolution of Flight and Immunity. *Science* **2013**, *339*, 456–460. [[CrossRef](#)]
30. Albrich, J.M.; McCarthy, C.A.; Hurst, J.K. Biological reactivity of hypochlorous acid: Implications for microbicidal mechanisms of leukocyte myeloperoxidase. *Proc. Natl. Acad. Sci. USA* **1981**, *78*, 210–214. [[CrossRef](#)]
31. Arnhold, J.; Monzani, E.; Furtmüller, P.G.; Zederbauer, M.; Casella, L.; Obinger, C. Kinetics and Thermodynamics of Halide and Nitrite Oxidation by Mammalian Heme Peroxidases. *Eur. J. Inorg. Chem.* **2006**, *2006*, 3801–3811. [[CrossRef](#)]
32. Davies, M.J.; Hawkins, C.L.; Pattison, D.I.; Rees, M.D. Mammalian Heme Peroxidases: From Molecular Mechanisms to Health Implications. *Antioxid. Redox Signal.* **2008**, *10*, 1199–1234. [[CrossRef](#)]
33. Slauch, J.M. How does the oxidative burst of macrophages kill bacteria? Still an open question. *Mol. Microbiol.* **2011**, *80*, 580–583. [[CrossRef](#)] [[PubMed](#)]
34. Aratani, Y. Myeloperoxidase: Its role for host defense, inflammation, and neutrophil function. *Arc. Biochem. Biophys* **2018**, *640*, 47–52. [[CrossRef](#)] [[PubMed](#)]
35. Beckman, J.S.; Beckman, T.W.; Chen, J.; Marshall, P.A.; Freeman, B.A. Apparent hydroxyl radical production by peroxynitrite: Implications for endothelial injury from nitric oxide and superoxide. *Proc. Natl. Acad. Sci. USA* **1990**, *87*, 1620–1624. [[CrossRef](#)] [[PubMed](#)]
36. McCafferty, D.M. Peroxynitrite and inflammatory bowel disease. *Gut* **2000**, *46*, 436–439. [[CrossRef](#)]
37. Radia, R. Oxygen radicals, nitric oxide, and peroxynitrite: Redox pathways in molecular medicine. *Proc. Natl. Acad. Sci. USA* **2018**, *115*, 5839–5848. [[CrossRef](#)] [[PubMed](#)]
38. Rowland, F.S. Nobel Lecture in Chemistry (1995).
39. Brasseur, G.P.; Orlando, J.J.; Tyndall, G.S. (Eds.) *Atmospheric Chemistry and Global Change*; Chapters 8 & 14; Oxford University Press: New York, NY, USA, 1999.
40. Molina, M.J.; Rowland, F.S. Stratospheric sink for chlorofluoromethanes: Chlorine atomic-catalysed destruction of ozone. *Nature* **1974**, *249*, 810–812. [[CrossRef](#)]
41. Ward, J.F. DNA Damage as the Cause of Ionizing Radiation-Induced Gene Activation. *Radiat. Res.* **1994**, *138*, S85–S88. [[CrossRef](#)]

42. Li, H.; Hu, J.; Xin, W.; Zhao, B. Production and interaction of oxygen and nitric oxide free radicals in PMA stimulated macrophages during the respiratory burst. *Redox. Rep.* **2000**, *5*, 353–358. [[CrossRef](#)]
43. Hazen, S.L.; Hsu, F.F.; Duffin, K.; Heinecke, J.W. Molecular Chlorine Generated by the Myeloperoxidase-Hydrogen Peroxide-Chloride System of Phagocytes Converts Low Density Lipoprotein Cholesterol into a Family of Chlorinated Sterols. *J. Biol. Chem.* **1996**, *271*, 23080–23088. [[CrossRef](#)]
44. Armesto, X.L.; Canle, L.M.; García, M.V.; Santaballa, J.A. Aqueous chemistry of N-halo-compounds. *Chem. Soc. Rev.* **1998**, *27*, 453–460. [[CrossRef](#)]
45. Dixon-Warren, S.J.; Jensen, E.T.; Polanyi, J.C. Photochemistry of adsorbed molecules. XI. Charge-transfer photodissociation and photoreaction in chloromethanes on Ag(111). *J. Chem. Phys.* **1993**, *98*, 5938–5953. [[CrossRef](#)]
46. Dixon-Warren, S.J.; Heyd, D.V.; Jensen, E.T.; Polanyi, J.C. Photochemistry of Adsorbed Molecules. XII. Photoinduced Ion-Molecule Reactions at a Metal Surface for CH₃X/RCl/Ag(111) (X=Br, I). *J. Chem. Phys.* **1993**, *98*, 5954–5960. [[CrossRef](#)]
47. Lu, Q.B.; Madey, T.E. Negative-ion enhancements in electron-stimulated desorption of CF₂Cl₂ coadsorbed with nonpolar and polar gases on Ru(0001). *Phys. Rev. Lett.* **1999**, *82*, 4122–4125. [[CrossRef](#)]
48. Lu, Q.B.; Sanche, L. Enhanced Dissociative Electron Attachment to CF₂Cl₂ by Transfer of Electrons Localized in Preexisting Traps of Water and Ammonia Ice. *Phys. Rev. B* **2001**, *63*, 153403. [[CrossRef](#)]
49. Wang, C.R.; Lu, Q.B. Real-time observation of a molecular reaction mechanism of aqueous 5-halo-2'-deoxyuridines under UV/ionizing radiation. *Angew. Chem. Intl. Ed.* **2007**, *46*, 6316–6321. [[CrossRef](#)] [[PubMed](#)]
50. Lu, Q.B. Effects of Ultrashort-Lived Prehydrated Electrons in Radiation Biology and Their Applications for Radiotherapy of Cancer. *Mutat. Res. Rev. Mutat. Res.* **2010**, *704*, 190–199. [[CrossRef](#)] [[PubMed](#)]
51. Stähler, J.; Gahl, C.; Wolf, M. Trapped Electrons on Supported Ice Crystallites. *Acc. Chem. Res.* **2012**, *45*, 131–138. [[CrossRef](#)]
52. Lind, J.; Jonsson, M.; Xinhua, S.; Eriksen, T.E.; Merenyi, G.; Ebersson, L. Kinetics of radical-initiated chain bromination of 2-methyl-2-propanol by N-bromosuccinimide in water. *J. Am. Chem. Soc.* **1993**, *115*, 3503–3510. [[CrossRef](#)]
53. Pattison, D.I.; O'Reilly, R.J.; Skaff, O.; Radom, L.; Anderson, R.F.; Davies, M.J. One-Electron Reduction of N-Chlorinated and N-Brominated Species Is a Source of Radicals and Bromine Atom Formation. *Chem. Res. Toxicol.* **2011**, *24*, 371–382. [[CrossRef](#)]
54. Vlasova, I.I. Peroxidase Activity of Human Hemoproteins: Keeping the Fire under Control. *Molecules* **2018**, *23*, 2561. [[CrossRef](#)]
55. Kee, T.K.; Son, D.H.; Kambhampati, P.; Barbara, P.F. A unified electron transfer model for the different precursors and excited states of the hydrated electron. *J. Phys. Chem. A* **2001**, *105*, 8434–8439. [[CrossRef](#)]
56. Nguyen, J.; Ma, Y.; Luo, T.; Bristow, R.G.; Jaffray, D.A.; Lu, Q.B. Direct observation of ultrafast electron transfer reactions unravels high effectiveness of reductive DNA damage. *Proc. Natl. Acad. Sci. USA* **2011**, *108*, 11778–11783. [[CrossRef](#)] [[PubMed](#)]
57. Chen, E.S.; Chen, E.C.; Sane, N. The electron affinities of the radicals formed by the loss of an aromatic hydrogen atom from adenine, guanine, cytosine, uracil, and thymine. *Biochem. Biophys Res. Commun.* **1998**, *246*, 228–230. [[CrossRef](#)] [[PubMed](#)]
58. Bankura, A.; Bankura, A.; Santra, B.; DiStasio, R.A., Jr.; Swartz, C.W.; Klein, M.L.; Wu, X. A systematic study of chloride ion solvation in water using van derWaals inclusive hybrid density functional theory. *Mol. Phys.* **2015**, *113*, 2842–2854. [[CrossRef](#)]
59. Adam, F.; Gosselain, P.A.; Goldfinger, P. Laws of Addition and Substitution in Atomic Reactions of Halogens. *Nature* **1953**, *171*, 704–705. [[CrossRef](#)]
60. Dixit, E.; Boulant, S.; Zhang, Y.; Lee, A.S.Y.; Odendall, C.; Shum, B.; Hacothen, N.; Chen, Z.J.; Whelan, S.P.; Fransen, M.; et al. Peroxisomes Are Signaling Platforms for Antiviral Innate Immunity. *Cell* **2010**, *141*, 668–681. [[CrossRef](#)]
61. Viggiano, A.A.; Arnold, F. Ion Chemistry and Composition of the Atmosphere. In *Handbook of Atmospheric Electrodynamics*; Volland, H., Ed.; Chapter 1; CRC Press: Boca Raton, FL, USA, 1995.
62. Viggiano, A.A. In situ mass spectrometry and ion chemistry in the stratosphere and troposphere. *Mass. Spectr. Rev.* **1993**, *12*, 115–137. [[CrossRef](#)]

63. Leach, J.K.; Tuyle, G.V.; Lin, P.S.; Schmidt-Ullrich, R.; Mikkelsen, R.B. Ionizing Radiation-induced, Mitochondria-dependent Generation of Reactive Oxygen/Nitrogen. *Cancer Res.* **2001**, *61*, 3894–3901.
64. Furtmüller, P.G.; Burner, U.; Obinger, C. Reaction of Myeloperoxidase Compound I with Chloride, Bromide, Iodide, and Thiocyanate. *Biochemistry* **1998**, *37*, 17923–17930. [[CrossRef](#)]
65. Furtmüller, P.G.; Burner, U.; Regelsberger, G.; Obinger, C. Spectral and Kinetic Studies on the Formation of Eosinophil Peroxidase Compound I and Its Reaction with Halides and Thiocyanate. *Biochemistry* **2000**, *39*, 15578–15584. [[CrossRef](#)]
66. Gao, J.; Tian, Z.; Yang, X. Breakthrough: Chloroquine phosphate has shown apparent efficacy in treatment of COVID-19 associated pneumonia in clinical studies. *Biosci. Trend* **2020**, *14*, 72–73. [[CrossRef](#)] [[PubMed](#)]
67. Touret, F.; de Lamballerie, X. Of chloroquine and COVID-19. *Antivir. Res.* **2020**, *177*, 104762. [[CrossRef](#)] [[PubMed](#)]
68. Yao, X.; Ye, F.; Zhang, M.; Cui, C.; Huang, B.; Niu, P.; Liu, X.; Zhao, L.; Dong, E.; Song, C.; et al. In Vitro Antiviral Activity and Projection of Optimized Dosing Design of Hydroxychloroquine for the Treatment of Severe Acute Respiratory Syndrome Coronavirus 2 (SARS-CoV-2). *Clin. Infect. Dis.* **2020**. [[CrossRef](#)] [[PubMed](#)]
69. Lu, Q.B.; Zhang, Q.R.; Ou, N.; Wang, C.R.; Warrington, J. In vitro and in vivo Studies of Non-Platinum-Based Halogenated Compounds as a New Class of Potent Antitumor Agents for Natural Targeted Chemotherapy of Cancers. *EBioMedicine* **2015**, *2*, 544–553. [[CrossRef](#)]
70. Wang, C.R.; Mahmood, J.; Zhang, Q.R.; Vedadi, A.; Warrington, J.; Ou, N.; Bristow, R.G.; Jaffray, D.A.; Lu, Q.-B. In Vitro and In Vivo Studies of a New Class of Anticancer Molecules for Targeted Radiotherapy of Cancer. *Mol. Cancer Ther.* **2016**, *15*, 640–650. [[CrossRef](#)]
71. Goetze, R.G.; Buchholz, S.M.; Ou, N.; Zhang, Q.; Patil, S.; Schirmer, M.; Singh, S.K.; Ellenrieder, V.; Hessmann, E.; Lu, Q.-B.; et al. Preclinical evaluation of 1,2-Diamino-4,5-dibromobenzene in genetically engineered mouse models of pancreatic cancer. *Cells* **2019**, *8*, 563. [[CrossRef](#)]
72. Schrezenmeier, E.; Dörner, T. Mechanisms of action of hydroxychloroquine and chloroquine: Implications for rheumatology. *Nat. Rev. Rheumatol.* **2020**, *16*, 155–166. [[CrossRef](#)]
73. Kaufmann, A.M.; Krise, J.P. Lysosomal Sequestration of Amine-containing Drugs: Analysis and Therapeutic Implications. *J. Pharm. Sci.* **2007**, *96*, 729–746. [[CrossRef](#)]
74. Ohkuma, S.; Poole, B. Fluorescence Probe Measurement of the Intralysosomal pH in Living Cells and the Perturbation of pH by Various Agents. *Proc. Natl. Acad. Sci. USA* **1978**, *75*, 3327–3331. [[CrossRef](#)]
75. Oda, K.; Koriyama, Y.; Yamada, E.; Ikehara, Y. Effects of Weakly Basic Amines on Proteolytic Processing and Terminal Glycosylation of Secretory Proteins in Cultured Rat Hepatocytes. *Biochem. J.* **1986**, *240*, 739–745. [[CrossRef](#)]
76. Hurst, N.P.; French, J.K.; Gorjatschko, L.; Betts, W.H. Chloroquine and Hydroxychloroquine Inhibit Multiple Sites in Metabolic Pathways Leading to Neutrophil Superoxide Release. *J. Rheumatol.* **1988**, *15*, 23–27. [[PubMed](#)]
77. Takeda, K.; Kaisho, T.; Akira, S. Toll-Like Receptors. *Ann. Rev. Immun.* **2003**, *21*, 335–376. [[CrossRef](#)] [[PubMed](#)]
78. Hayyan, M.; Hashim, M.A.; AlNashef, I.M. Superoxide Ion: Generation and Chemical Implications. *Chem. Rev.* **2016**, *116*, 3029–3085. [[CrossRef](#)] [[PubMed](#)]
79. Wang, C.R.; Lu, Q.B. Real-time observation of an ultrafast dissociative electron transfer reaction of a dihalogen-diamino-benzene molecule with the prehydrated electron. Unpublished.
80. Jorge, A.; Ung, C.; Young, L.H.; Melles, R.B.; Choi, H.K. Hydroxychloroquine retinopathy –implications of research advances for rheumatology care. *Nat. Rev. Rheumatol.* **2018**, *14*, 693–703. [[CrossRef](#)] [[PubMed](#)]
81. Caly, L.; Druce, J.D.; Catton, M.G.; Jans, D.A.; Wagstaff, K.M. The FDA-approved Drug Ivermectin inhibits the replication of SARS-CoV-2 in vitro. *Antiviral. Res.* **2020**. [[CrossRef](#)]

82. Ziegler, C.G.K.; Allon, S.J.; Nyquist, S.K.; Mbanjo, I.M.; Miao, V.N.; Tzouanas, C.N.; Cao, Y.; Yousif, A.S.; Bals, J.; Hauser, B.M.; et al. SARS-CoV-2 receptor ACE2 is an interferon-stimulated gene in human airway epithelial cells and is detected in specific cell subsets across tissues. *Cell* **2020**. [[CrossRef](#)]
83. Blanco-Melo, D.; Nilsson-Payant, B.E.; Liu, W.C.; Uhl, S.; Hoagland, D.; Møller, R.; Jordan, T.X.; Oishi, K.; Panis, M.; Sachs, D.; et al. Imbalanced host response to SARS-CoV-2 drives development of COVID-19. *Cell* **2020**, *181*, 1036–1045. [[CrossRef](#)]



© 2020 by the author. Licensee MDPI, Basel, Switzerland. This article is an open access article distributed under the terms and conditions of the Creative Commons Attribution (CC BY) license (<http://creativecommons.org/licenses/by/4.0/>).